

Journal of Materials Chemistry A

Accepted Manuscript



This is an *Accepted Manuscript*, which has been through the Royal Society of Chemistry peer review process and has been accepted for publication.

Accepted Manuscripts are published online shortly after acceptance, before technical editing, formatting and proof reading. Using this free service, authors can make their results available to the community, in citable form, before we publish the edited article. We will replace this *Accepted Manuscript* with the edited and formatted *Advance Article* as soon as it is available.

You can find more information about *Accepted Manuscripts* in the [Information for Authors](#).

Please note that technical editing may introduce minor changes to the text and/or graphics, which may alter content. The journal's standard [Terms & Conditions](#) and the [Ethical guidelines](#) still apply. In no event shall the Royal Society of Chemistry be held responsible for any errors or omissions in this *Accepted Manuscript* or any consequences arising from the use of any information it contains.

Cite this: DOI: 10.1039/c0xx00000x

www.rsc.org/xxxxxx

ARTICLE TYPE

Flexible Electrode Based on a Three-dimensional Graphene Network-supported Polyimide for Lithium-ion Batteries

Yuena Meng,^{a,b} Haiping Wu,^a Yajie Zhang,^a and Zhixiang Wei*^a*Received (in XXX, XXX) Xth XXXXXXXXX 20XX, Accepted Xth XXXXXXXXX 20XX*

DOI: 10.1039/b000000x

Flexible batteries are of great importance for the application of flexible electronic devices. In this paper, a flexible film electrode was designed and prepared by using three-dimensional graphene as a conductive network and polyimide (PI) as an active material. Structural characterizations indicate the formation of a uniform composite of PI and graphene. The weight ratio of the active material in the film electrode reaches 80%, and no additive is required during the electrode preparation processes. Compared with the electrode prepared by a conventional method, the hierarchical structure of graphene composited PI in the proposed electrode results in lower resistance for the reaction with lithium ions. PI exhibits a specific capacitance of 175 mAh·g⁻¹ as well as high rate performance. After 150 charge–discharge cycles at 0.5 C, 82% of the initial capacity was retained. This hierarchical graphene/PI film has high potential as a cathode for flexible lithium batteries.

Introduction

As clean and renewable energy-storage devices, lithium-ion batteries (LIBs) are currently used in plug-in hybrids, electric vehicles, and portable electronics. LIBs are considered as the most promising energy-storage devices for renewable energy because of their high energy density, long cycle life, and high efficiency.^{1,2} The properties of electrode materials are generally regarded as the determinant factor of LIB performance. In conventional LIBs, cathode materials are typically inorganic (e.g., LiCoO₂ and LiFePO₄).³ The movement of Li⁺ from and to the crystal structure during LIB charging and discharging results in kinetic problems. Moreover, the production and disposal of these materials cause pollution. Efforts are being made to develop high-performance but environment-friendly cathode materials.

As a strategy to meet the criteria for an electrode material, organic materials are used, which change the mechanism of lithium storage from intercalation to chemical bond reactions.⁴ The evolution of organic cathode materials started in the last century.⁵ Conducting polymers,⁶ organic sulfur compounds,⁷ and organic carbonyl compounds,⁸ among others, have all been used as electrode active materials. Of these compounds, organic materials based on the carbonyl group (e.g., anhydrides and quinones) have recently attracted considerable interest.⁹ Several types of polyimides (PIs) have been synthesized and analyzed as cathode materials,¹⁰ all of these PIs exhibit high discharge capacities and relatively long cycle life.

Nevertheless, the application of cathode materials generally depends on the formation of a three-dimensional (3D) electronic conductive network by carbon materials because both inorganic and organic active compounds generally do not conduct electrons.¹¹ Conventionally, significant amounts of

nanostructured carbon particles [e.g., carbon black (CB) and acetylene black] and polymer binders are used to construct electrodes. These carbon materials provide transport channels for electrons and also serve as a buffer to alleviate volume changes in the active material.¹² A typical organic electrode material requires more than 30 wt% of carbon material as well as binding additives.¹³ Both carbon materials and polymer binders do not contribute to capacity; therefore, their addition will reduce the overall capacity of the electrode.

Graphene has a large surface area and exhibits chemical stability as well as high electronic conductivity.¹⁴ Active materials are generally encapsulated with graphene to increase their electronic conductivity.^{15,16} However, graphene can form a connected conductive structure without other auxiliary materials because of its π – π stacking interactions.¹⁷ 3D graphene networks prevent the restacking of graphene sheets, provide pores for ion transport, and offer a low-density interconnected electrical conductive network,¹⁸ which is used as a unique supporting electrode for LIBs.¹⁹

In this study, we prepared a novel composite film electrode using an interconnected macroporous graphene network as the conductive network. PI, which is rich in carbonyl groups and exhibits a thermal stable structure, was used as the active material and was composited by in situ polymerization. Scheme 1 shows the molecular structure of PI. With this design, an electrode without binders was prepared. Moreover, the noncovalent conjugation interactions between the PI molecular structure and graphene provide sufficient contact for the optimal combination of ion- and electronic-conductive materials. This balanced combination reduces the electrode resistance and enhances the rate performance.

Experimental

Materials

Ethylene diamine (Sinopharm Chemical Reagent Co., China) was used without further purification. Pyromellitic dianhydride (Sinopharm Chemical Reagent Co., China) was used after reduced-pressure sublimation at 300 °C. Parachlorophenol (J&K Chemicals, China) was used as received.

Compositing of PI with 3D-RGO

The preparation of 3D-RGO is included in our previous report.²⁰

The film was further heat-treated in an argon atmosphere at 800 °C for 100 min to improve its conductivity. The synthesis route is shown in Scheme 1. A certain amount of parachlorophenol as solvent and monomer A (pyromellitic dianhydride) was placed in a vessel. One piece of the treated 3D-RGO film was then placed inside the reaction container. Then the vessel is heated until a clear yellow solution is formed. Afterward, monomer B (ethanediamine) was added into the vessel. The molar ratio of A to B was maintained at 1:1. The reaction system was subsequently heated to the desired temperature. The film was polymerized for 9 h, removed, washed with acetone and ethanol, and further heat-treated at 300 °C for 8 h in an Ar atmosphere.

Material characterization

The morphology was observed under SEM (HITACHI S-4800) and TEM (Tecnai G2 F20 U-TWIN). FT-IR spectral measurements were performed using a Perkin-Elmer Spectrum One spectrometer. The electrical conductivities of the films were determined using a Keithley instrument (Model 4200-SCS) via the four-probe method.

Lithium battery test

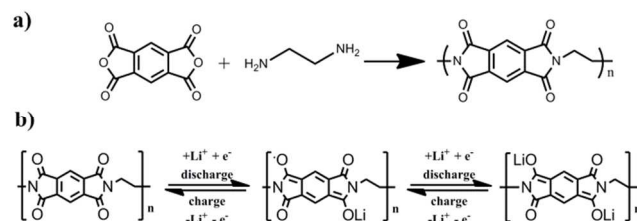
The composite film (marked as 3D-RGO/PI) was punched into round slices and directly used as an electrode. As for the PI-CB electrode, the same amount of active material (80 wt. % PI) used in 3D-RGO/PI was mixed with 15% CB and 5% PTFE. Ethanol was added to the mixture to form a slurry paste. The paste was rolled into pieces and punched into slices of the same size. Afterward, the electrodes were heated in a vacuum oven overnight at 60 °C.

The electrochemical performances were measured in Swagelok-type cells at room temperature, with the prepared electrode as the cathode. A 1 M LiTFSI DOL/DME solution was used as the electrolyte. Pure Al foil (Goodfellow) and glass fiber (Whatman) was used as the cathode current collector and separator, respectively. The galvanostatic charge/discharge tests were performed on an Arbin Instruments testing system in the 1.5 V to 3.5 V potential range. CV and EIS measurements were performed using a VMP3 electrochemical workstation.

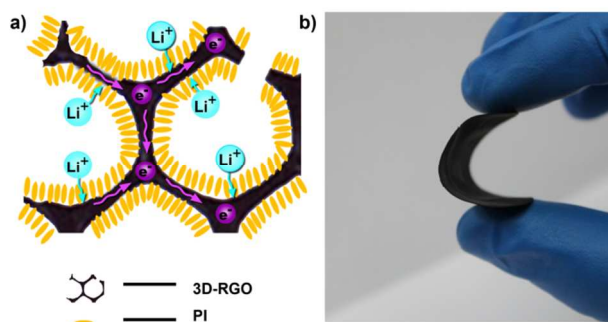
Results and discussion

3D graphene can be prepared by a template method by using graphene oxide, and then reduced into graphene by hydrazine (3D-RGO).²⁰ However, 3D-RGO acquires a large number of oxygen functional groups when reduced by hydrazine alone. Thus, 3D-RGO was heat-treated at 800 °C in the current study to improve its electrical conductivity. The Film resistance of 3D-

RGO decreased from approximately 82 $\Omega\cdot\text{sq}^{-1}$ to 21 $\Omega\cdot\text{sq}^{-1}$. The treated 3D-RGO film was composited with PI to obtain the composited film 3D-RGO/PI according to Scheme 1. Pyromellitic dianhydride and ethanediamine, which can readily diffuse to the interface of the graphene pores and the polymer, were used as monomeric molecular structures. A large number of conjugated carbonyl groups, which are beneficial for lithium storage,²¹ remain on the PI molecular structure (Scheme 1a). The structure of the composited film (Figure 1a) shows high flexibility (Figure 1b).



65 Scheme 1. (a) Synthesis and (b) reversible electrochemical mechanism of polyimide (PI).



70 Figure 1. (a) Schematic of the electrode with 3D graphene (3D-RGO) as the conductive network. (b) High bendable properties of the composite film.

The scanning electron microscopy (SEM) images of the 3D-RGO/PI composite film are shown in Figure 2. The interconnected macroporous structure can be clearly observed (Figure 2a). In the magnified images, nanoflakes with heights of approximately 100 nm to 200 nm are clearly observed on the graphene skeleton (Figures 2b to 2d). The PI nanoflakes are uniformly distributed on the surface of the interconnected graphene network. Moreover, the flakes are vertically aligned on graphene and are interlaced with one another. The mass ratio of PI was calculated as approximately 80% based on the weights of 3D-RGO and 3D-RGO/PI.

Transmission electron microscopy (TEM) characterization results (Figures 2e and 2f) also show the uniformity of the polymer coating on graphene. Figure 2f shows that the thickness of one PI nanoflake on graphene is about 5 nm to 8 nm. The uniform polymer coating is mainly attributed to the interconnected structure of 3D-RGO and the strong π - π interactions between the graphene surface and the PI backbones as a result of their conjugated aromatic rings.²²

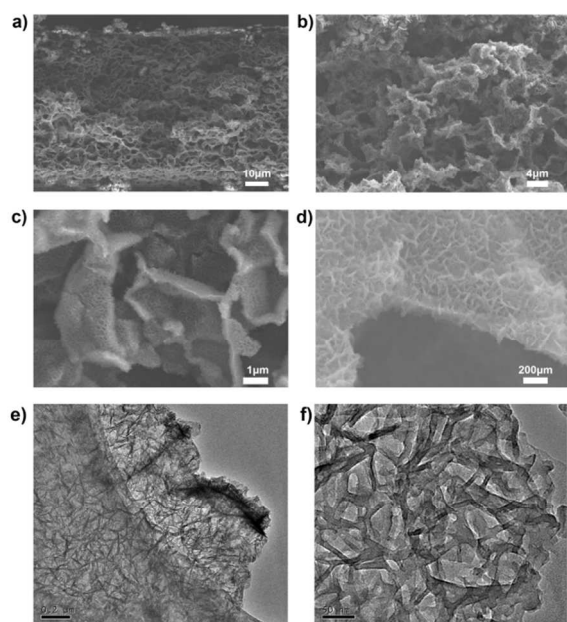


Figure 2. (a–d) Scanning electron microscopy (SEM) images of a 3D-RGO/PI cross-section at different magnifications. Vertically aligned polyimide (PI) nanoflakes are clearly observed on 3D-RGO. (e and f) Transmission electron microscopy (TEM) images of 3D-RGO/PI at different magnifications

Fourier transform infrared (FT-IR) spectroscopy further confirmed the combination of 3D-RGO and PI (Figure 3). The wide peak at 3453 cm^{-1} in the 3D-RGO spectrum is a characteristic absorption peak of hydroxyl. A similar peak is also observed on 3D-RGO/PI. Pure PI and the 3D-RGO/PI film both show boarder peaks at 1390 , 1723 , and 1775 cm^{-1} , which are assigned to the stretching vibration of C–N bond and to the asymmetric and symmetric stretching vibration of the C=O bond, respectively.¹⁰ 3D-RGO/PI shows the hybrid characteristics of the 3D-RGO and pure PI samples. This result implies that PI and 3D-RGO are successfully composited.

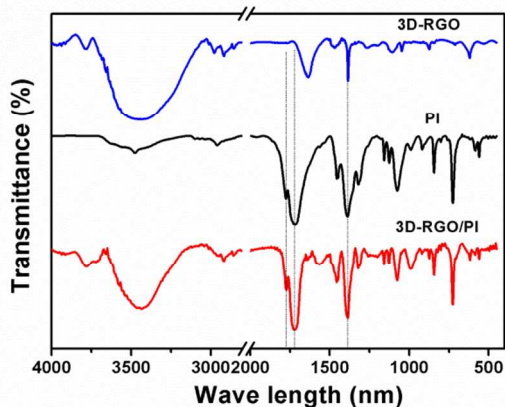


Figure 3. Fourier transform infrared (FT-IR) spectra of 3D-RGO, PI, and 3D-RGO/PI

The electrochemical performance of the 3D-RGO/PI composite film as an LIB cathode was investigated. For comparison, an electrode prepared by the conventional method, which was

prepared by mixing CB and PTFE (PI-CB) with PI at the same weight ratio as that in 3D-RGO/PI, was analyzed under the same conditions. The rate capabilities of 3D-RGO/PI and PI-CB-mixture electrodes with the same PI weight ratios were then compared. Their discharge current densities varied from 0.1 C to 5 C ($1\text{ C} = 443\text{ mAh}\cdot\text{g}^{-1}$) for 5 cycles at each rate and at a constant charge-current density.

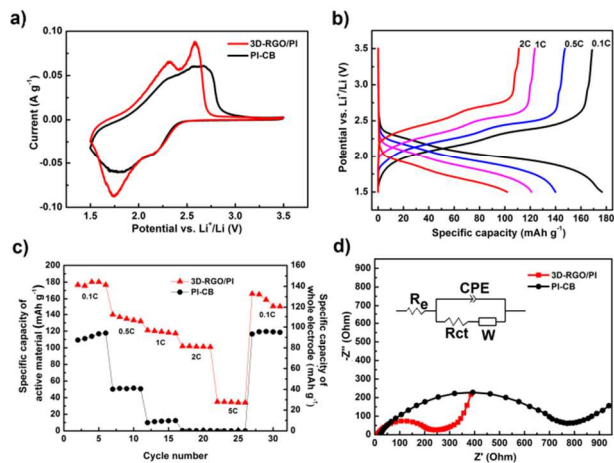


Figure 4. (a) Cyclic voltammetry (CV) curves for 3D-RGO/PI and PI-CB at $0.1\text{ mV}\cdot\text{s}^{-1}$. (b) Galvanostatic charging/discharging curves for 3D-RGO/PI. (c) Comparison of the rate capabilities of 3D-RGO/PI and PI-CB at different current densities. (d) Electrochemical impedance spectroscopy (EIS) of 3D-RGO/PI and PI-CB with equivalent inserted circuits.

The lithiation/delithiation behavior of 3D-RGO/PI was determined using cyclic voltammetry (CV) (Figure 4a). Above 1.5 V , two pairs of well-resolved redox peaks appear at 1.75 and 2.2 V as two reduction peaks and at 2.25 and 2.55 V as two oxidation peaks. This result indicates that two-electron transfer is involved in the behaviour. This finding is mainly due to the two continuous steps that successively produce a radical anion and a dianion (Scheme 1b). During this stage, PI displays a reversible capacity.²³ PI-CB shows similar peak positions but lower peak currents. These results indicate that 3D-RGO/PI exhibits a more effective electronic conductivity than PI-CB. In the charge/discharge profile (Figure 4b), the position of the voltage plateau is consistent with the CV curve peaks. The voltage and discharge capacities of the cells gradually decrease as the discharge current density increases. This trend explains the effect of polarization (i.e., IR drop) on the discharge performance. A discharge capacity of approximately $175\text{ mAh}\cdot\text{g}^{-1}$ is obtained at a discharge current density of 0.1 C . The average discharge plateau of the electrode is 2.07 V . The difference in the voltages of the charge and discharge plateaus is 88 mV at 0.1 C . These results indicate that the working voltage and the reversibility of 3D-RGO/PI are suitable for practical applications.^{10,24}

The specific capacities based on the masses of the active material and whole electrode are listed on the left and right side of Figure 4c, respectively. Figure 4c shows that the active material capacity of 3D-RGO/PI is $175\text{ mAh}\cdot\text{g}^{-1}$ at 0.1 C . When discharged at 2 C , the capacity remains at $101\text{ mAh}\cdot\text{g}^{-1}$, which indicates high rate performance. By contrast, the PI-CB electrode exhibits a capacity of only $120\text{ mAh}\cdot\text{g}^{-1}$ at 0.1 C . When the current density changes to 2 C , the discharge property nearly disappears. The discharge

capacities of PI-CB increasingly deteriorate compared with those of 3D-RGO/PI as the discharge current density increases to 5 C. This result demonstrates the high discharge-rate capability of 3D-RGO/PI. A high rate performance can be mainly attributed to sufficient contact between PI and 3D-RGO. 3D-RGO forms an effective conductive network, which guarantees effective electron conduction. Furthermore, the performance of the entire electrode is highly important in practical use. The entire 3D-RGO/PI electrode has a capacity of $140 \text{ mAh}\cdot\text{g}^{-1}$. By contrast, for an electrode with 60 wt.% of the active material, which is the most commonly used active material proportion in the conventional production of organic electrodes,^{25,26,27} $200 \text{ mAh}\cdot\text{g}^{-1}$ of the active material can only contribute $120 \text{ mAh}\cdot\text{g}^{-1}$ of capacity to the whole electrode.²⁸ Given the smaller weight ratio of its conductive part and the absence of a binder, the 3D-RGO/PI film electrode can deliver most of the PI energy, which is beneficial for practical use. In the subsequent discussion, the capacity of the entire electrode is used.

The electrochemical impedance spectroscopy (EIS) results for PI-CB and 3D-RGO/PI are shown in the form of Nyquist plots in Figure 4d. Equivalent electrical circuit results show similar R_e , namely, 19 and 17Ω . These results indicate electrolyte resistance. The resistance represents the charge-transfer (R_{ct}), which are 227Ω for 3D-RGO/PI and 745Ω for PI-CB. This finding indicates a significant difference in the electronic conductivities of the electrodes as well as in the interfacial charge transfers associated with ionic transport.^{18,29} The aforementioned result is consistent with that of the conductivity test. The electrical conductivities of 3D-RGO/PI and PI-CB are 1.84 and $0.34 \text{ S}\cdot\text{cm}^{-1}$, respectively. A high conductivity improves the rate performance. In addition, the high dispersion of 5 nm thick PI flakes on the RGO surface significantly shortens the diffuse distance of lithium ions.

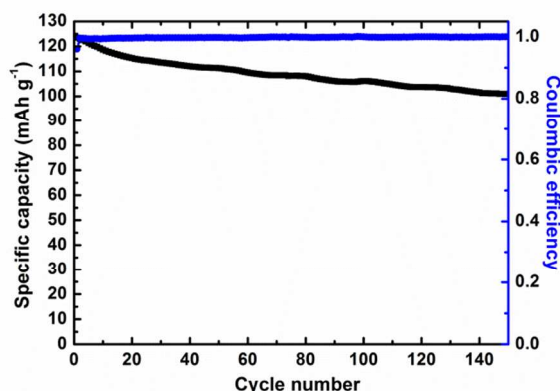


Figure 5. Capacity stability and coulombic efficiency of 3D-RGO during 150 charge/discharge cycles at 0.5 C.

Cycling stability is another important factor that determines the practical application of electrode materials. Figure 5a shows that 82% of the initial electrode capacity is preserved. The entire electrode can deliver an initial specific discharge capacity of $123 \text{ mAh}\cdot\text{g}^{-1}$, which decreases to $101 \text{ mAh}\cdot\text{g}^{-1}$ after 150 cycles at 0.5 C. The cycling stability of 3D-RGO/PI is higher than those of published reports.^[8] Moreover, the coulomb efficiency at all the aforementioned cycles is close to 100% and thus satisfies the basic criteria for cathode materials.

Conclusions

An effective 3D conductive network of graphene is produced and further used to fabricate a flexible composite electrode via in situ polymerization of PI. With this structure, the contact between the active material and the conductive network is more effective. Moreover, the formation of vertically aligned PI nanoflakes further optimizes the electrode performance. The composite can provide a specific capacitance of $175 \text{ mAh}\cdot\text{g}^{-1}$ based on the PI mass, or a specific capacitance of $140 \text{ mAh}\cdot\text{g}^{-1}$ based on the total mass of the electrode. Approximately 82% of the initial capacity is retained after 150 charge/discharge cycles at 0.5 C. This study proposes a facile strategy of producing a hierarchical electrode material with high flexibility and high potential application as a cathode for flexible lithium batteries.

Acknowledgments

This work was supported by the Ministry of Science and Technology of China (Grant Nos. 2010DFB63530, 2011CB932300, and 2009CB930400), the National Natural Science Foundation of China (Grant Nos. 21125420 and 91027031), and the Chinese Academy of Sciences.

Notes and references

- F. Cheng, J. Liang, Z. Tao and J. Chen, *Adv. Mater.*, 2011, 23, 1695-1715.
- V. Etacheri, R. Marom, R. Elazari, G. Salitra and D. Aurbach, *Energy Environ. Sci.*, 2011, 4, 3243-3262.
- G. Kucinskis, G. Bajars and J. Kleperis, *J. Power Sources*, 2013, 240, 66-79.
- L. Wang, D. Wang, F. Zhang and J. Jin, *Nano Lett.*, 2013, 13, 4206-4211.
- N. Oyama, T. Tatsuma, T. Sato and T. Sotomura, *Nature*, 1995, 373, 598-600.
- Y. Yang, C. Wang, B. Yue, S. Gambhir, C. O. Too and G. G. Wallace, *Adv. Energy Mater.*, 2012, 2, 266-272.
- Y. X. Yin, S. Xin, Y. G. Guo and L. J. Wan, *Angew. Chem. Int. Ed.*, 2013, 52, 13186-13200.
- H. Chen, M. Armand, M. Courty, M. Jiang, C. P. Grey, F. Dolhem, J. M. Tarascon and P. Poizot, *J. Am. Chem. Soc.*, 2009, 131, 8984-8988.
- H. Wu, K. Wang, Y. Meng, K. Lu and Z. Wei, *J. Mater. Chem. A*, 2013, 1, 6366.
- Z. Song, H. Zhan and Y. Zhou, *Angew. Chem. Int. Ed.*, 2010, 49, 8444-8448.
- S. Xin, Y. G. Guo and L. J. Wan, *Acc. Chem. Res.*, 2012, 45, 1759-1769.
- Y. Wu, Z. Wen, H. Feng and J. Li, *Chem. Eur. J.*, 2013, 19, 5631-5636.
- Y. Liang, P. Zhang and J. Chen, *Chemical Science*, 2013, 4, 1330-1337.
- Z. Chen, W. Ren, L. Gao, B. Liu, S. Pei and H. M. Cheng, *Nat. Mater.*, 2011, 10, 424-428.
- B. Lung-Hao Hu, F. Y. Wu, C. T. Lin, A. N. Khlobystov and L. J. Li, *Nat. Commun.*, 2013, 4, 1687.
- L. Wang, D. Wang, Z. Dong, F. Zhang and J. Jin, *Nano Lett.*, 2013, 13, 1711-1716.
- H. Jiang, P. S. Lee and C. Li, *Energy Environ. Sci.*, 2013, 6, 41-53.
- G. Zhou, L. C. Yin, D. W. Wang, L. Li, S. Pei, I. R. Gentle, F. Li and H. M. Cheng, *ACS Nano*, 2013, 7, 5367-5375.
- N. Li, Z. Chen, W. Ren, F. Li and H. M. Cheng, *Proc. Natl. Acad. Sci. USA*, 2012, 109, 17360-17365.
- Y. Meng, K. Wang, Y. Zhang and Z. Wei, *Adv. Mater.*, 2013.
- Z. Song and H. Zhou, *Energy Environ. Sci.*, 2013, 6, 2280-2301.

-
22. N. V. Kozhemyakina, J. M. Englert, G. Yang, E. Spiecker, C. D. Schmidt, F. Hauke and A. Hirsch, *Adv. Mater.*, 2010, 22, 5483-5487.
 23. Z. Song, H. Zhan and Y. Zhou, *Chem. Commun.*, 2009, 448-450.
 24. W. Choi, S. Ohtani, K. Oyaizu, H. Nishide and K. E. Geckeler, *Adv. Mater.*, 2011, 23, 4440-4443.
 - 5 25. P. C. Cheng, F. S. Tseng, C. T. Yeh, T. G. Chang, C. C. Kao, C. H. Lin, W. R. Liu, J. S. Chen and V. Zima, *CrystEngComm*, 2012, 14, 6812.
 26. M. Lee, J. Hong, D. H. Seo, D. H. Nam, K. T. Nam, K. Kang and C. B. Park, *Angew Chem Int Ed Engl*, 2013, 52, 8322-8328.
 - 10 27. J.-K. Kim, *J. Power Sources*, 2013, 242, 683-686.
 28. Z. Song, T. Xu, M. L. Gordin, Y. B. Jiang, I. T. Bae, Q. Xiao, H. Zhan, J. Liu and D. Wang, *Nano Lett.*, 2012, 12, 2205-2211.
 29. G. X. Wang, L. Yang, Y. Chen, J. Z. Wang, S. Bewlay and H. K. Liu, 15 *Electrochim. Acta*, 2005, 50, 4649-4654.

Table of contents

A flexible composite electrode for cathode of lithium battery is produced by compositing three-dimensional graphene network and vertically aligned polyimide nanoflakes.

